

ORIGINAL ARTICLE

In vivo study of the effect of combining endostatin gene therapy with ^{32}P -colloid on hepatocarcinoma and its functioning mechanism

Gao Huiqi¹, Zhu Jing², Fu Peng¹, Li Yong³, Shen Baozhong^{4,5}

¹Department of Nuclear Medicine, ²Department of Gerontology, ³Department of PET-CT, the First Affiliated Hospital of Harbin Medical University, Harbin, China; ⁴Department of Radiology, the Fourth Hospital of Harbin Medical University, Harbin, China;

⁵Molecular Imaging Research Center of Harbin Medical University, Harbin, China

Summary

Purpose: To investigate the therapeutic effect of combining ^{32}P colloid radiotherapy with endostatin anti-angiogenesis therapy on hepatocellular carcinoma (HCC) cells.

Methods: HCC mouse models were prepared using H22 cells and randomly divided into four groups. The mice were administered phosphate buffered saline (PBS), ^{32}P colloid, secretory endostatin encoding plasmid and combination of ^{32}P and endostatin, respectively. Seven, 14 and 21 days after treatment the mice were sacrificed. Expression of endostatin was confirmed using western blot. Tumor growth rate, microvessel density (MVD) in the solid tumor and apoptotic index (AI) of tumor cells was analyzed using immunohistochemistry and TUNEL methods.

Results: (1): From the western blot results, 1400 bp en-

dostatin specific protein bands were observed in the samples from groups 3 and 4, but not in the other two groups; (2): The tumor growth rate of groups 2, 3 and 4 was significantly decreased compared to group 1 and that of group 4 was significantly lower than group 2 and 3 (3): The MVD of group 1 was greatly higher than in the other groups (4): The AI of group 4 was dramatically higher than in the other groups.

Conclusions: ^{32}P colloid radiotherapy or endostatin anti-angiogenesis therapy were able to inhibit the growth of HCC cells in vivo, while the combination of ^{32}P and endostatin showed much better therapeutic effect in HCC treatment.

Key words: anti-angiogenesis, endostatin, hepatocarcinoma, ^{32}P colloid

Introduction

Accounting for 85-90% of all primary liver cancers, HCC ranks as the fifth most common primary cancer and the third leading cause of cancer-related deaths globally [1]. Currently, curative therapy options for HCC include surgical resection and liver transplantation [2]. However, due to the absence of early disease symptoms, rapid tumor progression and invasion-related spreading during early tumor stages, the prognosis for HCC is poor and only 10-20 % of patients are considered eligible for surgical treatment [3,4]. Thus there are great demands for novel therapeutic tac-

tics for HCC.

Radiotherapy has been widely used in various clinical malignant and pain management applications in the last 20 years [5,6]. It is able to deliver a highly concentrated absorbed dose to the targeted tumor while sparing the surrounding normal tissues. ^{32}P is a high-energy pure β -emitter with near ideal nuclear characteristics ($T_{1/2}$ of 14.3 days, moderately high energy of β - particles, maximum E_{β} of 1.71 MeV). Besides that, the low cost and abundant availability of ^{32}P makes it a promising therapeutic radioiso-

tope for tumors [7]. Extensive use of ^{32}P -chromic colloid for pleural and peritoneal effusions secondary to primary malignancies has been reported [8,9] and it has been approved by FDA as an antitumor radiopharmaceutical [10]. ^{32}P exhibits great antitumoral activity by inducing central tumor liquefaction [11]. Currently, technologic advances have provided the means to deliver tumoricidal doses of radiation therapy to patients with unresectable HCC, while avoiding critical normal tissues, providing the opportunity to use radiation therapy for curative intent treatment of HCC. However, angiogenic factors are upregulated in tumors in response to radiotherapy which might lead to tumor and endothelial radioresistance [12].

Consensus has been reached that solid tumors rely on angiogenesis for sustained growth and hematogenous metastatic spread [13,14]. Consequently, the concept of targeting the tumor vasculature with antiangiogenic agents has emerged as an attractive new strategy in the treatment of cancer [15-17]. Among these agents, endostatin, a 20 kDa C-terminal proteolytic fragment of collagen XVIII, has received the greatest attention [18]. Significant antitumor effects of endostatin have been reported in a variety of established tumor models of mouse, rat and human origins with low toxicity and acquired drug resistance [19-21]. However, antiangiogenic therapies, such as endostatin, cannot kill tumor cells directly. The greatest potential may be realized when used in conjunction with conventional therapies. HCC is a hypervascular tumor and angiogenesis plays a critical role in tumor growth and metastasis [22]. However, the research of endostatin combined with radiotherapy on HCC treatment is relatively limited.

This study investigated the therapeutic effect of the combination of ^{32}P colloid radiotherapy and endostatin anti-angiogenesis therapy on HCC using an orthotopic hepatoma mouse model. Specifically, HCC mouse models were prepared using H22 cells and were administered randomly PBS, as control, ^{32}P colloid, secretory endostatin encoding plasmid and combination of ^{32}P and endostatin, respectively. Mice were sacrificed at the 7th, 14th and 21st day after treatment. Expression of endostatin was firstly confirmed using western blot. The tumor growth rate, MVD and AI of tumor cells were further analyzed to evaluate the therapeutic effect on HCC.

Methods

Materials

The mouse hepatoma cell line H22 was purchased from Shanghai Institute of Cell Biology, Chinese Academy of Sciences. Four to six weeks old imprinting control region (ICR) mice, weighing 18-22 g were purchased from Shanghai Laboratory Animal Center, Chinese Academy of Science. All animals were maintained in pathogen-free conditions and handled in strict accordance with the PR China legislation of the use and care of laboratory animals. The plasmid encoding secretory endostatin was obtained from Beijing Medical University. ^{32}P colloid with diameter of 20-50 nm and radiopurity of 99% was purchased from Beijing Atomic Hi-Tech Co., LTD (Beijing, China).

HCC model preparation

Establishment of orthotopically implanted HCC mice model was established following the method described elsewhere [23]. Firstly, H22 cells were transferred into the abdominal cavity of an ICR mouse. After 6-8 days, the ascitic fluid was taken from the mouse and diluted with normal saline to a concentration of 1×10^7 cells/ml, and 0.2 ml was inoculated through subcutaneous injection at the right armpit of the mouse. They were then randomly divided into four groups (15 mice per group): (1) control group (saline), (2) ^{32}P group (intratumor injected with 0.3 mCi ^{32}P colloid), (3) endostatin group (intratumor injected with 20 μg secretory endostatin encoding plasmid) and (4) combination of ^{32}P and endostatin group. Another 5 HCC mouse models were prepared and sacrificed on the 7th day for the calculation of original tumor size (V_0).

Data collection

Seven, 14 and 21 days after treatment, HCC mouse models were sacrificed and tumors were segregated for the evaluation for therapeutic effects (5 mice per group each time).

Endostatin expression

The expression of endostatin in tissue homogenates from liver tumors subjected to different treatments was measured using western blot as described elsewhere [24].

Tumor growth rate

The tumor volume was monitored by measuring the tumor diameters in two dimensions. The tumor volumes were calculated as $V = L \times W^2 / 2$ (L: long diameter, W: short diameter) and tumor growth rate was determined as $f = V_t / V_0$ (V_t : the tumor volume at different time points, V_0 : the initial tumor volume).

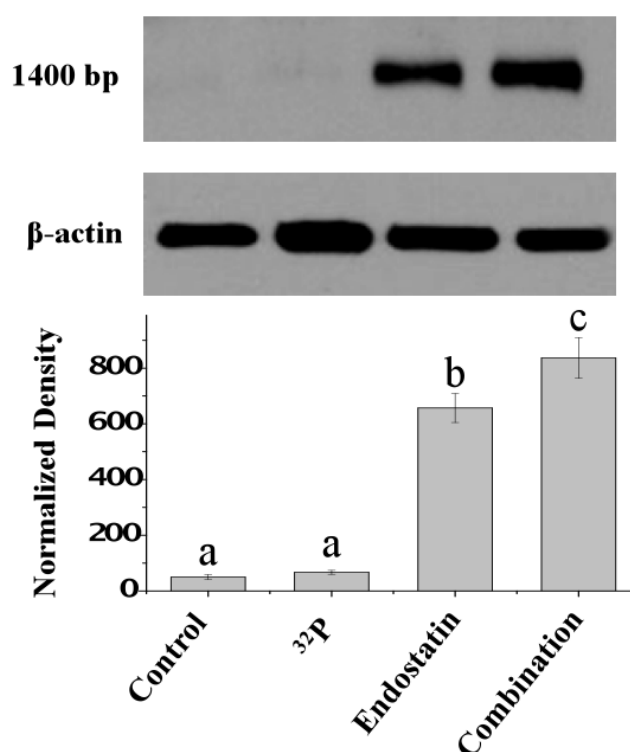


Figure 1. Western blot analysis of endostatin in homogenate of liver tumors from mice administered PBS, ^{32}P , endostatin, and combination of ^{32}P and endostatin for 21 days. Different letters indicate statistical difference (N=4, $p < 0.05$).

Table 1. Tumor growth rate (mean \pm standard deviation) in HCC mice models administrated with PBS (control), ^{32}P , endostatin and combination of ^{32}P with endostatin

Group	7 d	14 d	21 d
Control (PBS)	8.51 \pm 1.48	23.95 \pm 3.38	47.36 \pm 9.08
^{32}P	4.26 \pm 0.95*	15.68 \pm 2.34*	27.31 \pm 4.15*
Endostatin	6.18 \pm 0.86*	13.05 \pm 2.45*	21.63 \pm 4.20*
Combination	2.27 \pm 0.92*	4.38 \pm 1.34*	5.95 \pm 2.59*

*significant difference compared to control ($p < 0.01$), d: days

Microvessel density

Tumors were fixed in formalin and embedded in paraffin. The sections were then probed with a monoclonal rat anti-mouse CD31 antibody (Beckman, USA), followed by a biotinylated polyclonal rabbit anti-rat IgG antibody (Beckman, USA). The positive reaction was detected using the DAB substrate kit (Amresco, USA), and the sections were counterstained with hematoxylin. Finally, the microvessels were calculated with an Nikon microscope at x200 magnification.

Apoptotic index

The apoptotic cells in the tumor tissues were detected using the terminal deoxynucleotidyl trans-

ferase-mediated nick end labeling assay (TUNEL) (Sabc, Beijing, China) according to the manufacturer's instructions. Images were obtained by a Nikon fluorescence microscope at x200 magnification. The apoptotic cells were counted in 5 high power fields in each slide. The percentage of apoptotic cells among the total number of tumor cells defined the apoptotic index.

Statistics

Statistical analysis was performed using the SPSS software, version 16.0. The data were expressed as mean \pm SD, and significant differences were assessed using Student's *t*-test. $p < 0.05$ was considered statistically significant.

Table 2. Microvessel density in tumor sections and apoptotic index of tumor cells in HCC mice models administered PBS (control), ³²P, endostatin and combination of ³²P with endostatin

Group	MVD	AI
Control (PBS)	68.37 ± 12.62	5.08 ± 1.33
³² P	51.52 ± 8.87*	18.36 ± 2.42*
Endostatin	43.36 ± 8.02*	16.17 ± 2.14*
Combination	36.89 ± 5.71*	29.28 ± 3.01*

*significant difference compared to control (p<0.01). MVD: microvascular density, AI: apoptotic index, HCC: hepatocellular carcinoma

Results

Endostatin expression

To confirm the successful transfection of endostatin, the expression of endostatin in the homogenate of liver tumors 21 days after treatment was analyzed using western blot. A 1400 bp endostatin specific band was observed in the samples of the mice administered endostatin, or combination of ³²P and endostatin but could not be observed in control mice and mice administered ³²P colloid alone (Figure 1). Further, the amount of endostatin expressed in mice treated with combination of ³²p colloid and endostatin was significantly higher than those treated with endostatin alone. These results indicated that endostatin has been successfully transfected into liver tumors.

Tumor growth rate

Tumor growth rate was assessed to evaluate the tumor inhibitory effect of ³²P, endostatin, and combination of ³²P with endostatin. As shown in Table 1, tumor growth rate in the control group was 8.51±1.48, 23.95±3.38, 47.36±9.08 at the 7th, 14th and 21st day, respectively. In the irradiation group and endostatin plasmid injection group, the tumor growth rate was significantly slower than in the control group. Interestingly, the tumor growth rate in group 2 (³²P) was much slower than the growth in group 3 (endostatin) on the 7th day, but the value tended to be similar at the 14th and 21st day. In sharp contrast, the tumor growth rate in group 4 (combination of ³²P and endostatin) was dramatically slower than in the other three groups during the whole treating period with values of 2.27±0.92, 4.38±1.34 and 5.95±2.59 in the 7th, 14th and 21st day, respectively.

Microvessel density and apoptotic index

To evaluate the mechanism of the antitumor effect of ³²P, endostatin and combination of ³²P with endostatin, the intratumoral vascularization was assessed by immunohistology and MVD of tumor sections from different groups on the 21st day (Table 2). The MVD in mice administered PBS, ³²P, endostatin and combination of ³²P with endostatin was 68.37±12.62, 51.52±8.87, 43.36±8.02 and 36.89±5.71, respectively. The MVD of groups 2 and 3 was greatly decreased compared to the control. It decreased further when ³²P was combined with endostatin.

In order to estimate the apoptosis in tumor tissues, the tumor sections were stained with TUNEL reagent. Compared with the control group, the number of apoptotic cells was increased in the other groups and the AI is shown in Table 2 where it can be seen that the AI of tumor cells in groups 2 and 3 was significantly higher than that of the control group, and the highest index was obtained when combination of ³²P and endostatin was administered. This suggests that ³²P radiotherapy combined with endostatin inhibited the angiogenesis in tumors, which promoted increased apoptosis.

Discussion

HCC is the third most common type of cancer worldwide, causing over 370,000 deaths per year, with approximately half of them in China [25]. The complicated and unclear mechanism of HCC development makes the conventional therapy options, such as surgical treatment, chemotherapy and radiotherapy, unable to achieve satisfactory results. Since the middle of the last century, it has been realized that there is an important relation between tumor development/metastasis and angiogenesis. Tumor growth and metastases could be inhibited by angiogenesis inhibitors (e.g. endostatin) by specifically inhibiting endothelial proliferation and angiogenesis [26]. In our study, it was found that administration of endostatin in HCC mouse model was able to decrease the MVD in the solid tumor, contributing to slower tumor growth rate and higher AI. This result was consistent with the literature that endostatin inhibited Lewis lung carcinoma, fibrosarcoma, murine hemangioendothelioma (Eoma) and B16 melanoma, whose volume was about 100–200 mm³ [27].

The effect of endostatin is based on the inhibition of vascular bed formation by selectively suppressing the endothelial cell compartment within

a tumor, but overexpression of endostatin did not influence the morphology, proliferation, or migration of tumor cells. Therefore, combining conventional treatment strategies with endostatin might be the necessary way out to increase the overall efficacy of treatment [28]. Considering that angiostatin-mediated impairment of the tumor vasculature may restrict the access of the cytotoxic drugs to the tumor mass, regional radiotherapy appears better option than chemotherapy to be combined with endostatin treatment [26,29].

Preclinical data suggested that angiogenic factors are upregulated in tumors in response to radiotherapy [30] and the expression of proangiogenic factors is thought to be a potent survival factor that may lead to tumor and endothelial radioresistance [12,31]. In our study, the higher tumor growth rate in 14th and 21st day compared to the 7th day was possibly due to the upregulation of angiogenic factors after ^{32}P irradiation treatment. However, when ^{32}P treatment was combined with anti-angiogenesis treatment using endostatin, the tumor growth rate remained low during the treatment period. It was suggested that endothe-

lial cell proliferation is increased in tumors after irradiation but is blocked by the concurrent administration of endostatin, and the combination of endostatin with radiation enhances endothelial cell apoptosis. In our study, when the combination of ^{32}P and endostatin was applied on tumor bearing mice, the AI of tumor cells was significantly larger than in the control group and when only radiotherapy or endostatin were used. These observations were consistent with other reports that exposure of the cells to 2Gy gamma-rays reduced the time to reach the maximum expression level of endostatin and also increased the amount of secreted endostatin protein ($p < 0.001$) [32]. These can be explained hypothesizing that the expression of vascular endothelial growth factor, interleukin-8, and matrix metalloproteinase-2 are increased after irradiation in tumors, and this increase is blocked by endostatin [31].

^{32}P colloid radiotherapy or endostatin anti-angiogenesis therapy were able to inhibit the growth of liver tumor *in vivo*, while the combination of ^{32}P and endostatin showed much better therapeutic effect in HCC treatment.

References

1. Lau W, Lai E. The Current Role of Radiofrequency Ablation in the Management of Hepatocellular Carcinoma. A Systematic Review. *Ann Surg* 2009;249:20-25.
2. Sotiropoulos GC, Molmenti EP, Loesch C, Beckebaum S, Broelsch CE, Lang H. Meta-analysis of tumor recurrence after liver transplantation for hepatocellular carcinoma based on 1,198 cases. *Eur J Med Res* 2007;12:527-534.
3. Tang Z-Y, Ye S-L, Liu Y-K et al. A decade's studies on metastasis of hepatocellular carcinoma. *J Cancer Res Clin Oncol* 2004;130:187-196.
4. Song T-J, Wai Kit Ip E, Fong Y. Hepatocellular carcinoma: Current surgical management. *Gastroenterology* 2004;127(5, Suppl):S248-S260.
5. Hoefnagel C. Radionuclide therapy revisited. *Eur J Nucl Med* 1991;18:408-431.
6. Ersahin D, Doddamane I, Cheng D. Targeted Radionuclide Therapy. *Cancers* 2011;3:3838-3855.
7. Singh A, Holmes RA, Farhangi M et al. Human pharmacokinetics of samarium-153 EDTMP in metastatic cancer. *J Nuclear Med* 1989;30:1814-1818.
8. Denis-Bacelar AM, Romanchikova M, Chittenden S et al. Patient-specific dosimetry for intracavitary P-32-chromic phosphate colloid therapy of cystic brain tumours. *Eur J Nucl Med Mol Imag* 2013;40:1532-1541.
9. Sonett JR, Ginsburg ME, Javidfar J et al. Lung-sparing Ambulatory Repeated Intrapleural Chemotherapy Plus Intrapleural P-32 Isotope Radiation for Malignant Pleural Mesothelioma. *J Thor Oncol* 2010;5:S513-S514.
10. Prabhakar G, Sachdev SS, Umamaheswari S et al. Development of samarium [32P] phosphate colloid for radiosynoviorthesis applications: Preparation, biological and preliminary clinical studies experience. *Appl Radiat Isotop* 2007;65:1309-1313.
11. Rosemurgy A, Luzardo G, Cooper J et al. 32P as an Adjunct to Standard Therapy for Locally Advanced Unresectable Pancreatic Cancer: A Randomized Trial. *J Gastrointest Surg* 2008;12:682-688.
12. Kumar P, Miller AI, Polverini PJ. p38 MAPK Mediates γ -Irradiation-induced Endothelial Cell Apoptosis, and Vascular Endothelial Growth Factor Protects Endothelial Cells through the Phosphoinositide 3-Kinase-Akt-

- Bcl-2 Pathway. *J Biol Chem* 2004;279:43352-43360.
13. Folkman J. Tumor angiogenesis: therapeutic implications. *NEJM* 1971;285:1182-1186.
 14. Wong MLH, Prawira A, Kaye AH, Hovens CM. Tumor angiogenesis: Its mechanism and therapeutic implications in malignant gliomas. *J Clin Neurosci* 2009;16:1119-1130.
 15. Zhang Y, Yu L-K, Lu G-J et al. Prognostic Values of VEGF and Endostatin with Malignant Pleural Effusions in Patients with Lung Cancer. *Asian Pacific J Cancer Prev* 2014;15:8435-8440.
 16. Ren Z, Wang Y, Jiang W, Dai W, Jiang Y. Anti-Tumor Effect of a Novel Soluble Recombinant Human Endostatin: Administered as a Single Agent or in Combination with Chemotherapy Agents in Mouse Tumor Models. *Plos One* 2014. 9(9).
 17. Winlaw DS. Angiogenesis in the pathobiology and treatment of vascular and malignant diseases. *Ann Thor Surg* 1997;64:1204-1211.
 18. O'Reilly MS, Boehm T, Shing Y et al. Endostatin: An endogenous inhibitor of angiogenesis and tumor growth. *Cell* 1997;88:277-285.
 19. Berger AC, Feldman AL, Gnant MFX et al. The Angiogenesis Inhibitor, Endostatin, Does Not Affect Murine Cutaneous Wound Healing. *J Surg Res* 2000;91:26-31.
 20. Peroulis I, Jonas N, Saleh M. Antiangiogenic activity of endostatin inhibits C6 glioma growth. *Int J Cancer* 2002;97:839-845.
 21. Li XP, Li CYS, Li XH et al. Inhibition of human nasopharyngeal carcinoma growth and metastasis in mice by adenovirus-associated virus-mediated expression of human endostatin. *Mol Cancer Ther* 2006;5:1290-1298.
 22. Ueda K, Terada T, Nakanuma Y, Matsui O. Vascular supply in adenomatous hyperplasia of the liver and hepatocellular carcinoma: a morphometric study. *Hum Pathol* 1992;23:619-626.
 23. Jia HJ, Li Y, Zhao TS et al. Antitumor effects of Stat3-siRNA and endostatin combined therapies, delivered by attenuated Salmonella, on orthotopically implanted hepatocarcinoma. *Cancer Immunol Immunother* 2012;61:1977-1987.
 24. Li X-P, Zhang H-L, Wang H-J et al. Ad-endostatin treatment combined with low-dose irradiation in a murine lung cancer model. *Oncol Rep* 2014;32:650-658.
 25. Wang JX, Zhang LY, Zhang J, Ding H, Wang DM, Wang ZP. The synergistic effect of organic silicone quaternary ammonium salt and 5-fluorouracil on hepatocellular carcinoma in vitro and in vivo. *Eur J Cancer Prev* 2014;23:372-384.
 26. Shibata MA, Morimoto J, Doi H, Morishima S, Naka M, Otsuki Y. Electrogenic therapy using endostatin, with or without suicide gene therapy, suppresses murine mammary tumor growth and metastasis. *Cancer Gene Ther* 2006;14:268-278.
 27. Wu D-S, Wu C-M, Huang T-H, Xie Q-D. Combined effects of radiotherapy and endostatin gene therapy in melanoma tumor model. *Radiat Environm Biophys* 2008;47:285-291.
 28. Zhuang H-Q, Yuan Z-Y. Process in the mechanisms of endostatin combined with radiotherapy. *Cancer Lett* 2009;282:9-13.
 29. Hebert C, Siavash H, Norris K, Nikitakis NG, Sauk JJ. Endostatin inhibits nitric oxide and diminishes VEGF and collagen XVIII in squamous carcinoma cells. *Int J Cancer* 2005;114:195-201.
 30. Gorski DH, Beckett MA, Jaskowiak NT et al. Blockade of the vascular endothelial growth factor stress response increases the antitumor effects of ionizing radiation. *Cancer Res* 1999;59:3374-3378.
 31. Itasaka S, Komaki R, Herbst RS et al. Endostatin improves radioresponse and blocks tumor revascularization after radiation therapy for A431 xenografts in mice. *Int J Radiat Oncol Biol Phys* 2007;67:870-878.
 32. Luo X, Andres ML, Timiryasova TM, Fodor I, Slater JM, Gridley DS. Radiation-enhanced Endostatin Gene Expression and Effects of Combination Treatment. *Technol Cancer Res Treat* 2005;4:193-201.